Journal of Materials and Environmental Sciences
ISSN : 2028-2508
CODEN : JMESCN

J. Mater. Environ. Sci., 2018, Volume 9, Issue 4, Page 1165-1169

https://doi.org/10.26872/jmes.2018.9.4.128

http://www.jmaterenvironsci.com

Synthesis and characterization of new pyrochlore solid solutions(1-x) $Gd_2Sn_2O_7$ – x MO (M = Mg or Zn)

M. Douma[1], K. Haboubi[1], E.H. Chtoun[2], K. Andaloussi[3]

[1] *Laboratory of Engineering Science and Application, National School of Applied Sciences of Al-Hoceima, Morocco*
[2] *Laboratory Of Solid Chemistry, Faculty of Sciences, Abdelmalek Essaadi University, Tetouan, Morocco*
[3] *Laboratory of Water, Studies and Environmental Analysis, Department of Chemistry, Faculty of science, Abdelmalek Essaadi University*

Received 01 Jun 2017,
Revised 12Dec 2017,
Accepted 14 Dec 2017

Keywords
- ✓ Mixed oxide,
- ✓ Pyrochlore structure,
- ✓ Solid solutions,

m.douma@yahoo.fr ;
Phone:+212666881277.

Abstract

The study of the binary system (1-x) $Gd_2Sn_2O_7$ – x MO (M = Mg and Zn) shows new solid solutions with pyrochlore structure. They were synthesized using a conventional ceramic method and characterized by X-ray diffraction (XRD) and Fourier transform infrared (FT-IR) absorption spectroscopy. The results showed that the resulting phases are new non stoichiometric solid solutions with the pyrochlore type structure in the compositional range $0 \leq x \leq 0{,}38$ for M = Mg and $0 \leq x \leq 0{,}43$ for M = Zn. The evolution of the lattice parameter, *a, of* these solid solutions decreases when the degree of substitution, *x*, increases in both series.

1. Introduction

The $A_2B_2O_7$ overall formula for ideal oxide pyrochlores is often written as $A_2B_2O_6O'$ to distinguish the oxygen atoms (or anions) in the two different networks. This structure can be described in the space group *Fd-3m (No. 227)* with*Z = 8*, that is commonly referred as a fluorite derivative. The A cations, occupying the *(16d)* sites (using Wyckoff's notation) [1], are coordinated to eight oxygen atoms. The smaller B cations occupy the *(16c)* sites and are coordinated to six oxygen atoms at equal distances in trigonal antiprism. The O atoms (On the *48f*sites) are at (*x*, 0.125, 0.125) and are bonded to two A and two B atoms. The O' atom is bonded only to A atoms [1].The crystal phase stability of $A_2B_2O_7$ can be determined by the r_{A3+}/r_{B4+} ratio of cations radii [2]. Usually, the ordered pyrochlore structure lies in the range of $1.46 \leq r_A/r_B \leq 1.80$. If r_A/r_B exceeds 1.80, the ordered pyrochlore structure is nolonger the stable phase for $A_2B_2O_7$ materials. If r_A/r_B is below 1.46, thedisordered defect-fluorite structure forms.

These mixed metal oxides have been extensively studied, especially there ionic, electrical, magnetic, magneto-caloric and vibrational properties [3].Because of their ability to accept rare earth chemical elements in solid solutions and their chemical stability; they have even been proposed as matrices to immobilize highly radioactive waste [4,5].

Pyrochlore-type stannates $A_2^{3+}Sn_2^{4+}O_7$ where the A cation is a trivalent rare earth raised a particular interest. According to previous studies [6], they exhibit catalytic activities and high-temperature stabilities in various reaction processes and they have been shown to be a series of potential phosphor materials [7]. Recent interests in stannates pyrochlores have stemmed from their highly efficient oxidative coupling of methane and their potential uses as high-temperature gas sensors and fast ion conductors [8]. Other important characteristic of the pyrochlore type oxides is the anionic conductivity that is related to the oxygen stoichiometry [9]. In defect structures conductivity depends on oxygen jumps between neighboring anionic sites within the BO_6octahedra and AO_6 sheets [10]. This behavior has been attributed to the presence of vacancies which are intrinsic structural features of these materials.

In a previous work[11] we have reported the preparation of new solid solutions in the binary system (1-x) $A_2Sn_2O_7$ – x MO (A = Eu, Y and M = Mg, Zn) with pyrochlore structure. This kind of solids is normally obtained by the conventional ceramic method, but recently they also obtained by microwave hydrothermal synthesis[12, 13].In other works[2, 14, 15] we have determinate the structure of these solid solutions by Rietveld analysis. The aim of present work is to explore new binaries systems with pyrochlore structure.

2. Material and Methods

2.1. Experimental

Solid solutions of (1-x) $Gd_2Sn_2O_7$ – x MO (M = Mg, Zn) with compositions x = 0, 0.15, 0.2, 0.25, 0.3, 0.35, 0.4, 0.45, 0.5, 0.6, were prepared using the conventional mixed oxide method in two steps. The principal is based on mixing the starting materials Gd_2O_3, SnO_2 and MO (M=Mg, Zn) (all reagents from Aldrich) in powder form. Quantities corresponding to the desired compositions were finely ground and carefully mixed in an agate mortar and then placed in alumina crucibles. This mixture is heat-treated to provide the necessary energy for interdiffusion of the oxides and crystallization of the pyrochlore phase. The whole is heated to 1000 °C for 48 hours in a muffle furnace (heating rate is 10 °C/min) then at 1400 °C for 96 hours after a new grinding. Samples obtained after slow cooling were systematically weighed before and after reaction. No mass variation was detected.

2.2. X-ray diffraction

X-ray powder diffraction patterns were recorded with a Siemens D-500 diffractometer using Cu-K*α(λ= 1.5405 Å)* radiation. The goniometer was connected to a PC controlled by the commercial program DACO-MP. The powder diffraction pattern was obtained by scanning with counting steps of 1.5 s, from 12º to 85 º 2θ using 0.05 step-intervals.

2.3. FT-IR spectroscopy

The Fourier-transformed infrared (FT-IR) spectra were recorded in a Perkin-Elmer FT-IR-1600 spectrometer at a nominal resolution of 4 cm^{-1} and averaging 16 scans to improve the signal-to-noise ratio. Each sample was diluted in IR-grade potassium bromide and pressed into self-supported discs.

3. Results and discussion

X-ray diffraction patterns analysis of the compositions prepared in the two systems showed the existence of a single phase of pyrochlore structure for compounds rich in $Gd_2Sn_2O_7$. All the diffraction peaks could be readily indexed to the pure phase of $Gd_2Sn_2O_7$, *JCPDS-130186*. No impurity peaks such as those of SnO_2, Gd_2O_3, MgO or ZnO are detected. Since they all have cubic crystal system with *Fd-3m* space group.

The evolution of the lattice parameter as a function of the composition, x, is plotted in Figures1 and 2. This parameter decreases gradually when the content of MO (M = Mg, Zn) increases and reaches a lower limiting value 38% for (1-x) $Gd_2Sn_2O_7$ – x MgOand 43% for (1-x) $Gd_2Sn_2O_7$ – x ZnO. Beyond these compositions the lattice parameter has constant remainder and there is appearance of two phases field: solid solution with pyrochlore structure and MO (M = Mg, Zn). The two compositions thus correspond to the limits of the homogeneity field of the binary solid solutions.

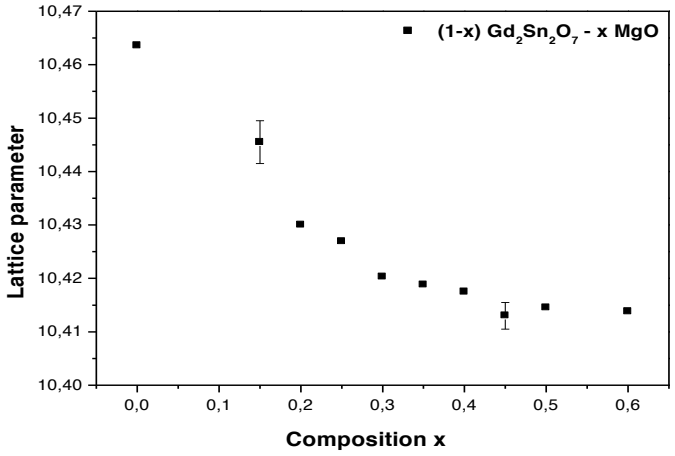

Figure 1: lattice parameter *(a)* evolution according to the composition*(x)* of (1-x) $Gd_2Sn_2O_7$ – x MgO solid solution.

Figures3 and 4 show the powder X-ray diffraction patterns of some prepared compositions. The overlay of these patterns shows clearly a great analogy between the stoichiometric $Gd_2Sn_2O_7$ phase pattern and those of some compositions prepared in the two systems. The expansion of some regions of these overlay patterns reveals the shift to higher θ values of the phases which contain the MO oxide (M = Mg, Zn) with respect to the stoichiometric $Gd_2Sn_2O_7$ phase, which also explains the decrease of the lattice parameter (Figures5 and 6).

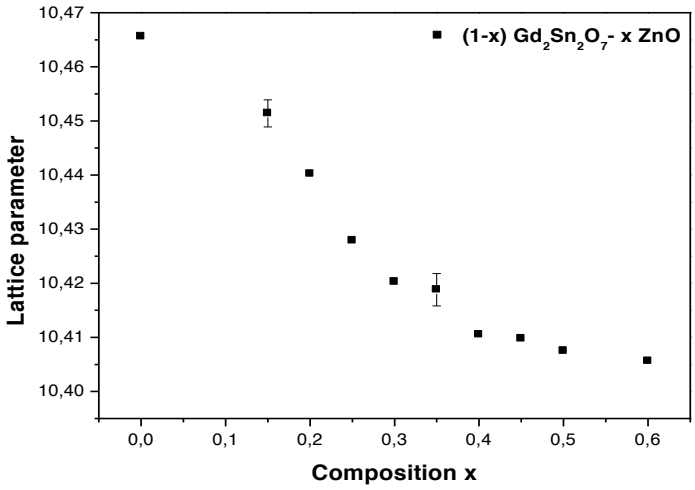

Figure 2: lattice parameter*(a)* evolution according to the composition*(x)* of (1-x) $Gd_2Sn_2O_7$ – x ZnO solid solution.

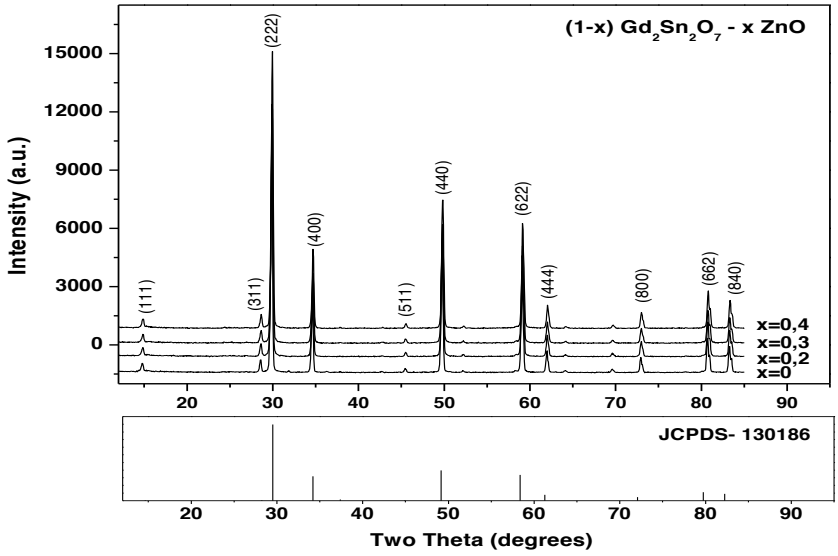

Figure 3: Powder XRD patterns of some prepared compositions of (1-x) $Gd_2Sn_2O_7$ – x ZnO solid solution.

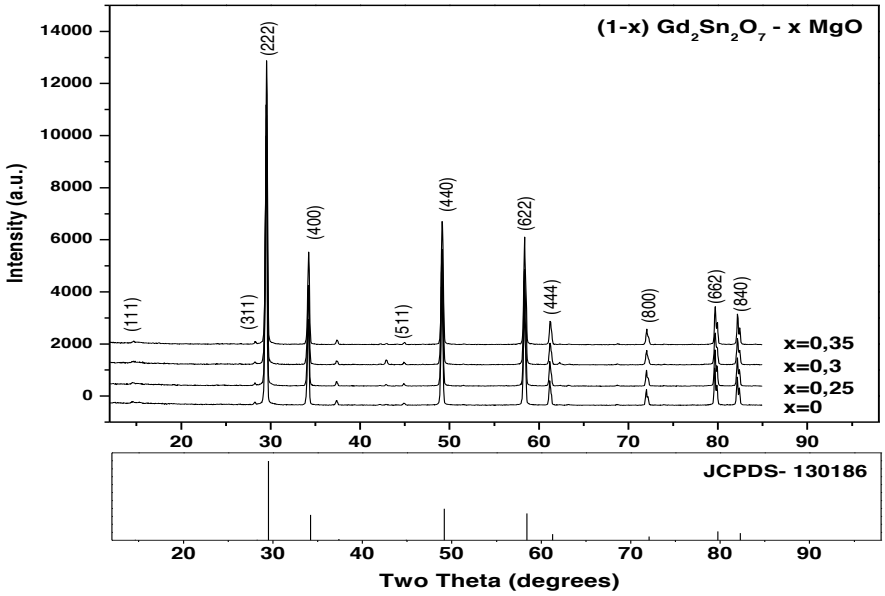

Figure 4: Powder XRD patterns of some prepared compositions of (1-x) $Gd_2Sn_2O_7$ – x MgO solid solution.

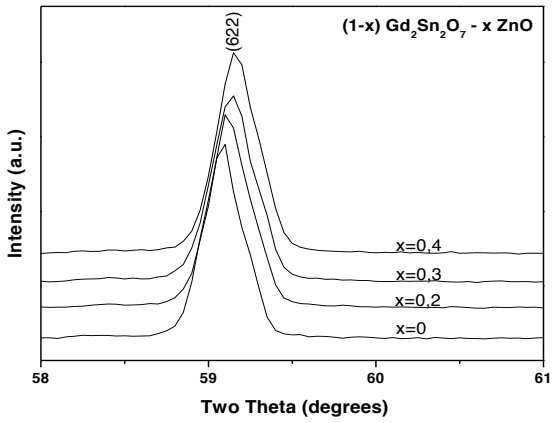

Figure 5: Shift observed in the (622) peak for (1-x) $Gd_2Sn_2O_7$ – x ZnO solid solution.

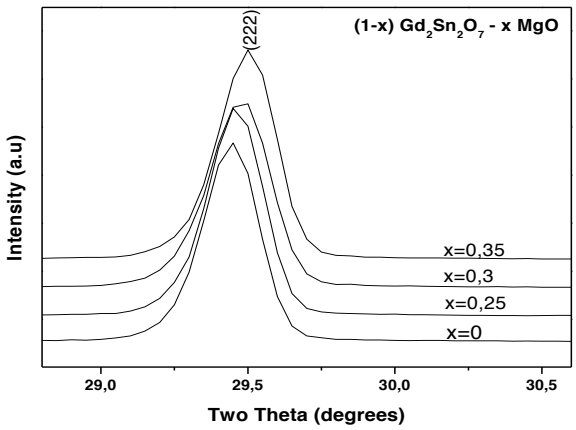

Figure 6: Shift observed in the (222) peak for (1-x) $Gd_2Sn_2O_7$ – x MgO solid solution.

From (1-x) $Gd_2Sn_2O_7$ – x MO, the solid solution can be formulated: $(Gd_{2-x}M_x)Sn_2O_{7-x/2}$. This formula shows the existence of the additional vacancies in the cationic and anionic sublattices compared to the general formula $Gd_2Sn_2O_7$. A study of structural analysis using Rietveld methodis in hand to more precise the structure of these solid solutions.

When a M^{2+} ion replaces a Gd^{3+} ion at A site in $Gd_2Sn_2O_7$, this will lead to a positive charge deficiency in the compound. Hence, anionic vacancies must be created to balance the positive charge deficiency of the compound. The effective ionic radius of eight coordinated Gd^{3+}, Mg^{2+} and Zn^{2+} ions are 1.05 Å, 0.89 Å and 0.9 Å respectively [16]. The ratio of the average effective ionic radii of the Gd^{3+} and M^{2+} ions to the one of Sn^{4+} ion for the two solid solutions are listed in Table 1. It has suggested [17] that the pyrochlore structure will only be favored if the r_{A3+}/r_{B4+} radii ratio is in the range of 1.46-1.80. In our case the criterion was carried out for the two solid solutions. The presence of pyrochlore compound with formula $(Gd_{2-x}M_x)Sn_2O_{7-x/2}$ (M = Mg, Zn) is possible.

Table 1: ratio of the average effective ionic radii of the Gd^{3+} and M^{2+} ions to the one of Sn^{4+} ion for the two solid solutions.

	$(Gd_{2-x}Mg_x)Sn_2O_{7-x/2}$; 0 ≤x≤ 0.38	$(Gd_{2-x}Zn_x)Sn_2O_{7-x/2}$; 0 ≤x≤ 0.43
x	rA^{3+}/rB^{4+}	rA^{3+}/rB^{4+}
0	1.5217	1.5217
0.15	1.5043	1.5054
0.20	1.4985	1.5000
0.25	1.4927	1.4945
0.30	1.4869	1.4891
0.35	1.4811	1.4836
0.40	-	1.4782
0.45	-	1.4728

The FT-IR spectra were recorded on polycrystalline powders in the form of KBr discs from 4000 to 400 cm^{-1}. There are seven characteristic absorption bands in the region 1200-100 cm^{-1} for the pyrochlore compounds with the general formula $A_2B_2O_7$[18] but those below 400 cm^{-1} cannot be recorded with our instrument. Figures7 and 8show the FT-IR spectra of (1-x) $Gd_2Sn_2O_7$ – x MO in the 1000 - 400 cm^{-1} range. The band close to 600 cm^{-1} is due to the B-O stretching vibration in the BO_6 octahedron and the band around 400 cm^{-1} is assigned to the A-O' stretching vibration. It can be seen from the Figures 7and 8 that all spectra of the synthesized solid solutions are similar to those observed in the $Gd_2Sn_2O_7$ pyrochlore structure, suggesting that the M^{2+} cations are well distributed in the pyrochlore structure. The strong band observed in the region 700-600 cm^{-1} for all compositions can be ascribed to Sn-O stretching vibration [19].

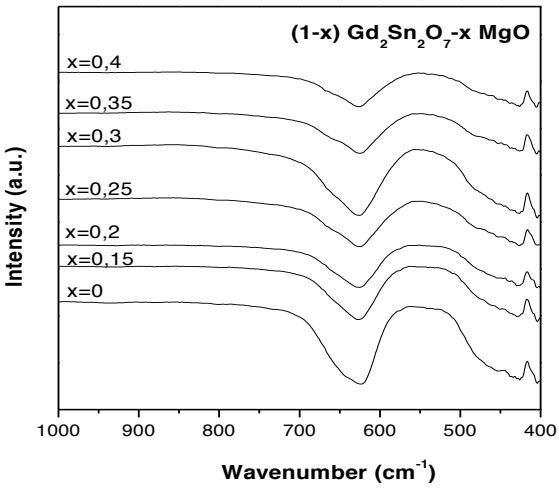

Figure 7: FT-IR spectra of (1-x) $Gd_2Sn_2O_7$ – x MgO solid solution.

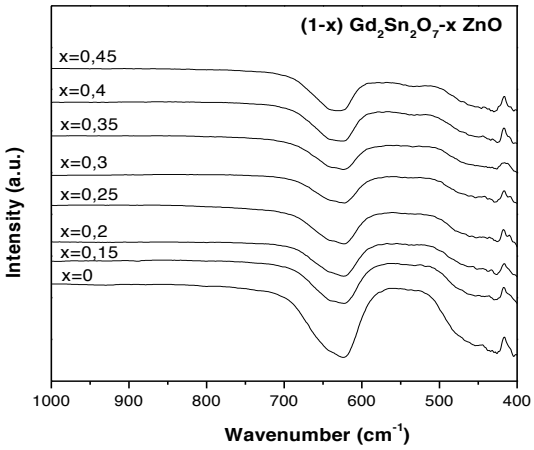

Figure 8: FT-IR spectra of (1-x) $Gd_2Sn_2O_7$ – x ZnO solid solution.

Conclusion

This study enabled us to underline new solid solutions with the pyrochlore structure: (1-x) $Gd_2Sn_2O_7$ – x MgO and (1-x) $Gd_2Sn_2O_7$- x ZnO. All phases prepared are characterized by X-ray diffraction and Fourier transform infrared spectroscopy. X-ray diffraction (XRD) analysis confirmed that these pyrochlores crystallize in cubic symmetry, space group *Fd-3m*. The field of homogeneity was specified and it is wider in the case of the solid solutions with ZnO than in that with MgO. For bothseries the introduction of the M (M=Mg, Zn) cation into the pyrochlore decreased the cell parameter as compared to the $Gd_2Sn_2O_7$structure.The distribution of the M^{2+} cations in the pyrochlore structure was confirmed by the FT-IR analysis. A structural analysis, by Rietveldmethod is in hand to determinate the exact formula of these solid solutions.

References

1. A.M. Srivastava, *Opt. Mater.*3 1 (2009) 881-885.
2. M. Douma, E.H. Chtoun, R. Trujillano, V. Rives, *Mater. Res. Bull*. 45 (2010) 29-33.
3. S. Nandi, Y.M. Jana, D. Swamakar, J. Alam, P. Bang, R. Nath, *J. Alloy. Comp*. 714 (2017) 318-370.
4. Z. Huang, J.Qi, M. Zhou, Y. Gong, Q. Shi, M. Yang, W. Han, Z.K. Cao, S. Peng, T. Lu, *Ceram. Int*. 44, Issue 2.1 (2018) 1334-1342.
5. J. Wang, W. Junxia, Y. Zhang, Y. Li,Y. Teng, Z. Wang, H. Tan, *Ceram. Int.* 43 (2017) 17064-17070.
6. B.A. Hunter, C.J. Howard, *J. Solid State Chem*. 130 (1997) 58-65.
7. A. Zych, A. Reinhardt, B. Albert, *J. Alloy. Comp*. 723 (2017)30-35.
8. Yachun Mao, Guangshe Li, Wei Xu and Shouhua Feng, *J. Mater. Chem*. 10 (2000) 479-482.
9. A. Garbout, S. Bouattour, M. Ellouze, A.W. Kolsi, *J. Alloy. Comp*. 425 (2006) 88-95.
10. M. Pirzada, R.W. Grimes, L. Minervini, J.F. Maguire, K.E. Sickafus, *Solid State Ionics*. 140 (2001) 201-208.
11. M. Douma, E.H. Chtoun, R. Trujillano, V. Rives, S. Khayroun, *Ann. Chim. Sci. Mater*. 34 (2009) 21-26.
12. R. Trujillano, V. Rives, M.Douma.E.H. Chtoun, *Ceram. Int*. 41 (2015) 2266-2270.
13. J. Liao, L.Nie, Q. Wang, S.Liu, J.Fu, H.R. Wen, *J. Lumin*. 183 (2017) 377-382.
14. R. Trujillano, M. Douma, E.H.Chtoun, V. Rives, *Macla*. 11 (2009) 187-188.
15. M. Douma, E.H. Chtoun, R.Trujillano, V. Rives, *Process. Appl. Ceram*. 4[4] (2010) 237-243.
16. R.D. Shannon, *Acta Crystallogr.*A 32 (1976) 751.
17. F. Brisse, D.J. Stewart, V. Seidl, O. Knop, *Can. J. Chem*. 50 (1972) 3648.
18. T.T. Zhang, K.W. Li, J. Zeng, Y.L. Wang, X.M. So,g, H. Wang, *J. Phys. Chem. Solids*. 69 (2008) 2845-2851.
19. J. Cheng, H. Wang, Z. Hao, S. Wang, *Catal.Commun*.9 (2008) 690.

(2018) ;http://www.jmaterenvironsci.com